

环境科学

(HUANJING KEXUE)

ENVIRONMENTAL SCIENCE

第38卷 第9期

Vol.38 No.9

2017

中国科学院生态环境研究中心 主办
科学出版社 出版



目次

中国国道和省道机动车尾气排放特征 王人洁,王堃,张帆,高佳佳,李悦,岳涛(3553)

北偏西大风对北京冬季生物气溶胶的影响 闫威卓,王步英,Oscar Fajardo Montana,蒋靖坤,郝吉明(3561)

不同空气质量等级下环境空气颗粒物及其碳组分变化特征 方小珍,吴琳,张静,李怀瑞,毛洪钧,宋从波(3569)

大气颗粒物及降尘中重金属的分布特征与人体健康风险评价 王永晓,曹红英,邓雅佳,张倩(3575)

2014年6月南京大气复合污染观测 郝建奇,葛宝珠,王自发,张祥志,汤莉莉,徐丹卉(3585)

嘉兴市不同天气条件下大气污染物和气溶胶化学组分的分布特征 王红磊,沈利娟,唐倩,吕升,田旭东,李莉,张孝寒(3594)

应用扩散管测量霾污染期间大气氮硫化合物浓度的方法 田世丽,刘学军,潘月鹏,周焱博,许稳,王跃思(3605)

福建省地级市人为源活性氮排放及其特征分析 张千湖,高兵,黄蕙,颜晓妹,崔胜辉(3610)

珠三角某高校室内灰尘重金属含量水平、来源及其健康风险评价 蔡云梅,黄涵书,任露陆,张艳林(3620)

贵金属和助剂负载量对柴油公交车 CDPF 颗粒净化性能的影响 谭丕强,仲益梅,郑源飞,楼狄明,胡志远(3628)

东营市北部海域沉积物中重金属的分布、来源及生态风险评价 刘群群,孟范平,王菲菲,崔鸿武,王曰杰(3635)

基于 MERIS 影像的洪泽湖叶绿素 a 浓度时空变化规律分析 刘阁,李云梅,吕恒,牟蒙,雷少华,温爽,毕顺,丁潇蕾(3645)

太湖蠡河小流域水质的空间变化特征及污染源解析 连慧姝,刘宏斌,李旭东,宋挺,雷秋良,任天志,武淑霞,李影(3657)

黄河高村至利津河段水体和沉积物中不同形态磷的分布特征 赵瞰,贾雁翔,姜兵琦,梅翔宇,李敏(3666)

三峡澎溪河流域消落区与岸边土壤磷形态特征 黄俊杰,王超,方博,冯磊,方芳,李哲,郭劲松(3673)

网湖沉积物正构烷烃分布特征及其记录的环境变化 沈贝贝,吴敬禄,曾海鳌,张永东,金苗(3682)

高地下水位地区透水停车场的水文控制效果 金建荣,李田,王圣思,陈子隼,周佳雯(3689)

北方典型设施蔬菜种植区地下水水质特征 于静,虞敏达,蓝艳,何小松,李敏(3696)

垃圾填埋水溶性有机物组成、演化及络合重金属特征 肖骁,何小松,席北斗,高如泰,李丹,张慧,崔东宇,袁志业(3705)

潜流人工湿地基质结构与微生物群落特征的相关性 李振灵,丁彦礼,白少元,李雪芬,游少鸿,解庆林(3713)

滑石矿开采对着生藻群落结构和水环境的影响 臧小苗,张远,林佳宁,王书平,高欣,赵茜,王靖淇(3721)

高铵条件下绿狐尾藻的生理与氮磷吸收特征 刘少博,冉彬,曾冠军,李宝珍,朱红梅,刘锋,肖润林,吴金水(3731)

活性炭吸附对藻类有机物的去除及其消毒副产物的控制 苗雨,翟洪艳,于珊珊,张婧,史常香(3738)

石墨烯凝胶电极的制备及电吸附 Pb^{2+} 的性能 王瑶,吉庆华,李永峰,胡承志(3747)

电流密度对 BDD 电极电化学矿化吡啶的影响与机制 张佳维,王婷,郑彤,蒋欢,倪晋仁(3755)

黄铁矿光化学氧化降解微囊藻毒素-LR 的机制 周薇,方艳芬,张钰,吴春红,黄应平(3762)

双氧水协同生化法强化处理印染废水 岳秀,唐嘉丽,于广平,吉世明,刘竹寒(3769)

基于 ABR-MBR 组合工艺不同进水 C/N 比对反硝化除磷性能的影响机制 吴鹏,程朝阳,沈耀良,赵诗惠,吕亮(3781)

利用好氧颗粒污泥持续增殖启动高性能亚硝化反应器 高军军,钱飞跃,王建芳,陈希,沈耀良,张泽宇,闫俞廷(3787)

零价铁自养反硝化过程活性污泥矿化及解决措施 张宁博,李祥,黄勇,张文静(3793)

低氧污泥丝状菌膨胀的呼吸图谱特征分析 马智博,李志华,杨成建,贺春博,秋亮,张晶(3801)

市政污泥接种焦化废水好氧降解能力及微生物群落演替的响应分析 刘国新,吴海珍,孙胜利,胡肖怡,吴晓英,陈华勇,范一文,胡成生,韦朝海(3807)

高效反硝化细菌的快速培养及群落结构多样性分析 孟婷,杨宏(3816)

两座污水处理系统中细胞态和游离态抗生素抗性基因的丰度特征 张衍,陈吕军,谢辉,李奥林,代天娇(3823)

生物炭对土壤 CH_4 、 N_2O 排放的影响 周凤,许晨阳,王月玲,林云,王强,张彤彤,耿增超(3831)

江西省耕地土壤碳氮比空间变异特征及其影响因素 江叶枫,郭熙,孙凯,饶磊,李婕,王澜珂,叶英聪,李伟峰(3840)

碳酸钙与生物炭对酸化菜地土壤持氮能力的影响 俞映惊,杨林章,Alfred Oduor Odindo,薛利红,何世颖,段婧婧(3851)

黄土丘陵区小流域不同整地措施长期影响下的土壤水力学特性 冯天骄,卫伟,陈利顶,陈蝶,干洋,杨磊(3860)

有机碳含量对多环芳烃在土壤剖面残留及迁移的影响 费佳佳,张枝焕,万甜甜,何奉朋(3871)

酸雨区不同用地类型土壤有效态 Cd 含量季节变化及关键影响因子 刘孝利,曾昭霞,铁柏清,叶长城,周俊驰,雷鸣(3882)

陕西潼关冶金污染土壤的修复评价及应用潜力 王姣,肖然,李荣华,宁西翠,蒋顺成,李晓龙,张增强,沈锋(3888)

甘肃白银东大沟铅锌镉复合污染场地水泥固化稳定化原位修复 吕浩阳,费杨,王爱勤,阎秀兰,李发生,李春萍,杜延军,郑梓铭(3897)

设施栽培对土壤与蔬菜中 PAHs 污染特征及其健康风险评价 金晓佩,贾晋璞,毕春娟,王薛平,郭雪,陈振楼,仇新莲(3907)

镉-铅复合污染下 AM 真菌对玉米生长和镉、铅吸收的影响 常青,郭伟,潘亮,王起凡,周昕南,杨亮,李娥(3915)

秸秆还田对水稻镉积累及其亚细胞分布的影响 段桂兰,王芳,岑况,王伯勋,程旺大,刘跃川,张红梅(3927)

Pantoea sp. IMH 介导土壤中砷的形态转化 张林,卢金锁(3937)

生物炭对土壤中重金属铅和锌的吸附特性 王红,夏雯,卢平,布雨薇,杨浩(3944)

浒苔生物炭的特征及其对 Cr(VI) 的吸附特点和吸附机制 陈友媛,惠红霞,卢爽,王报英,王志婕,王楠(3953)

灼烧净水污泥对外源磷的吸附和固定作用 于胜楠,李勇,李大鹏,黄勇(3962)

污泥生物炭制备吸附陶粒 李杰,潘兰佳,余广炜,汪印,尤甫天,谢胜禹(3970)

石墨相氮化碳-碘氧化铋层状异质结的构建及其光催化杀菌性能 黄建辉,林文婷,谢丽燕,陈建琴(3979)

《环境科学》征稿简则(3859) 《环境科学》征订启事(3952) 信息(3644, 3688, 3768)

利用好氧颗粒污泥持续增殖启动高性能亚硝化反应器

高军军¹, 钱飞跃^{1,3,4}, 王建芳^{1,2,3,4*}, 陈希¹, 沈耀良^{1,3,4}, 张泽宇¹, 闫俞廷²

(1. 苏州科技大学环境科学与工程学院, 苏州 215009; 2. 苏州科技大学天平学院, 苏州 215009; 3. 城市生活污水资源化利用技术国家地方联合工程实验室, 苏州 215009; 4. 江苏省环境科学与工程重点实验室, 苏州 215009)

摘要: 为了考察亚硝化颗粒污泥(NGS)的持续增殖能力,向柱状序批式反应器(SBR)内接种极少量种污泥,在130 d内,将氨氮容积负荷(NLR)从 $0.74 \text{ kg} \cdot (\text{m}^3 \cdot \text{d})^{-1}$ 提高到 $6.66 \text{ kg} \cdot (\text{m}^3 \cdot \text{d})^{-1}$,成功使反应器内污泥浓度(MLSS)从 $0.1 \text{ g} \cdot \text{L}^{-1}$ 增长至 $11.8 \text{ g} \cdot \text{L}^{-1}$,对应的亚硝态氮累积负荷从 $0.4 \text{ kg} \cdot (\text{m}^3 \cdot \text{d})^{-1}$ 升至 $4.9 \text{ kg} \cdot (\text{m}^3 \cdot \text{d})^{-1}$. 当NLR低于 $4.44 \text{ kg} \cdot (\text{m}^3 \cdot \text{d})^{-1}$ 时,反应器内粒径 $<200 \mu\text{m}$ 的污泥数量明显增多,颗粒平均粒径大幅减小. 当NLR继续提高时,颗粒平均粒径的增长过程遵循修正的Logistic模型,其比增长速率 k 值约为 0.0229 d^{-1} . 在运行期间,较高的游离氨(FA)和游离亚硝酸(FNA)浓度能够对亚硝酸盐氧化菌(NO_B)起到联合抑制作用,这使得出水中亚硝态氮累积率(NAR)始终高于80%. 上述实验结果将为工业化高效NGS反应器的启动操作提供重要参考.

关键词: 好氧颗粒污泥; 亚硝化反应; 序批式生物反应器; 氨氮负荷; 污泥增殖

中图分类号: X703.1 文献标识码: A 文章编号: 0250-3301(2017)09-3787-06 DOI: 10.13227/j.hjkk.201703194

Start-up of a High Performance Nitrosation Reactor Through Continuous Growth of Aerobic Granular Sludge

GAO Jun-jun¹, QIAN Fei-yue^{1,3,4}, WANG Jian-fang^{1,2,3,4*}, CHEN Xi¹, SHEN Yao-liang^{1,3,4}, ZHANG Ze-yu¹, YAN Yu-ting²

(1. School of Environmental Science and Engineering, Suzhou University of Science and Technology, Suzhou 215009, China; 2. Tianping College, Suzhou University of Science and Technology, Suzhou 215009, China; 3. National and Local Joint Engineering Laboratory of Municipal Sewage Resource Utilization Technology, Suzhou 215009, China; 4. Jiangsu Key Laboratory of Environmental Science and Engineering, Suzhou 215009, China)

Abstract: In order to examine the continuous growth capacity of the nitrosation granular sludge (NGS), the sludge was inoculated to start up the columnar sequencing batch reactor (SBR). During 130 d, the concentration of mixed liquor suspended solids (MLSS) in SBR increased from $0.1 \text{ g} \cdot \text{L}^{-1}$ to $11.8 \text{ g} \cdot \text{L}^{-1}$, corresponding to the nitrite-nitrogen accumulation rate of 0.4 – $4.9 \text{ kg} \cdot (\text{m}^3 \cdot \text{d})^{-1}$, promoted by a higher ammonia-nitrogen loading rate (NLR) from $0.74 \text{ kg} \cdot (\text{m}^3 \cdot \text{d})^{-1}$ to $6.66 \text{ kg} \cdot (\text{m}^3 \cdot \text{d})^{-1}$ in the influent. Because of the obvious increase in small granules (size $<200 \mu\text{m}$), the mean average diameter of NGS decreased significantly at $\text{NLR} < 4.44 \text{ kg} \cdot (\text{m}^3 \cdot \text{d})^{-1}$. At higher NLR values, the growth of the mean average diameter of NGS could be fitted well using a modified logistic model. The specific growth rate of the k value was 0.0229 d^{-1} . In addition, the combined inhibition of nitrite oxidizing bacteria (NO_B) was expected at relatively high concentrations of both free ammonia (FA) and free nitrite acid (FNA); thus, the nitrite accumulation ratio (NAR) in the effluent was always higher than 80%. These results provide a feasible approach to start up a high-performance NGS reactor at the industrial-scale.

Key words: aerobic granular sludge; nitrosation; sequencing biological reactor; ammonia loading rate; sludge growth

众所周知,亚硝化反应是运行亚硝化-厌氧氨氧化工艺(SHARON-ANAMMOX)、短程硝化-反硝化工艺等新型生物脱氮工艺的技术基础和限制性步骤^[1,2]. 有研究表明,培养沉降性能优良、表面基质梯度分布的好氧颗粒污泥,有利于同时对氨氧化菌(AOB)的富集和对亚硝酸盐氧化菌(NO_B)的抑制,该技术是获得稳定、高效亚硝化反应的可行途径之一^[3]. 但与典型异养菌相比,AOB的最大生长速率更小($\mu_{\text{max,异养菌}}$ 为 $4 \sim 8 \text{ d}^{-1}$, $\mu_{\text{max,AOB}}$ 为 $0.6 \sim 1.0 \text{ d}^{-1}$)、细胞产率更低 [$Y_{\text{max,异养菌}}$ 为 $0.5 \sim 0.7 \text{ g} \cdot \text{g}^{-1}$ (以 COD/COD 计), $Y_{\text{max,AOB}}$ 为 $0.10 \sim 0.12$

$\text{g} \cdot \text{g}^{-1}$ (以 $\text{VSS}/\text{NH}_4^+ \text{-N}$ 计)]、自凝聚能力也更差^[4]. 同时,在活性污泥系统中,AOB与NO_B存在紧密的共生关系,需要通过对溶解氧、温度、游离氨浓度等关键参数的准确调控,才能做到对后者的选择性抑制或淘洗^[5,6]. 因此,培养全自养型亚硝化颗粒污

收稿日期: 2017-03-22; 修订日期: 2017-04-10

基金项目: 国家自然科学基金项目(51308367,51578353); 苏州科技大学研究生科研创新计划项目(SKCX16-022,SKCX16-032); 江苏高校优势学科建设项目; 江苏省高校大学生实践创新训练计划项目(201613985003Y)

作者简介: 高军军(1991~),男,硕士研究生,主要研究方向为废水生物处理理论与技术,E-mail:405412145@qq.com

* 通信作者,E-mail:wj302@163.com

泥(NGS)的难度要远高于异养型好氧颗粒污泥。

目前,NGS反应器的启动方法主要有两种:①接种絮状污泥,在低C/N比条件下,同步实现亚硝化与污泥颗粒化功能^[7,8];②接种异养型好氧颗粒污泥,通过基质负荷调控,实现污泥亚硝化功能^[9,10]。在实际工程中,通过接种少量种污泥,并利用其增殖过程启动生化反应器也是常用的方法,但该技术路线能否用于高性能NGS反应器的启动仍有待验证。

鉴于此,本研究在NGS初始浓度仅为 $0.1 \text{ g}\cdot\text{L}^{-1}$ 的条件下,尝试启动小试规模的序批式反应器(SBR)。以氨氮容积负荷(NLR)为推动力,保持较高的水力剪切与排水比,成功实现了颗粒污泥的快速增殖。在此期间,对反应器氮转化效能、污泥增殖规律与功能菌活性变化也进行了系统分析,相关结论对于推动NGS反应器的工程化应用具有重要意义。

1 材料与方法

1.1 接种污泥

接种污泥(NGS)取自实验室小试规模的SBR反应器。反应器进水采用无机人工配水。当NLR为 $1.6 \text{ kg}\cdot(\text{m}^3\cdot\text{d})^{-1}$ 时,SBR对氨氮的去除率大于95%,出水亚硝态氮累积率(NAR)约为90%。NGS呈红棕色,平均粒径 $1400 \mu\text{m}$,污泥沉降指数(SVI值)为 $17 \text{ mL}\cdot\text{g}^{-1}$ 。

1.2 实验装置

实验装置采用有机玻璃制成的圆柱型SBR反应器,高径比为10/1,有效容积为4L,装置参见文献[11]。接种污泥(MLSS)浓度为 $0.1 \text{ g}\cdot\text{L}^{-1}$ 。反应器底部设有曝气头,反应期间曝气量设定为 $2.5 \text{ L}\cdot\text{min}^{-1}$,对应的表观上升气速可达 $1.1 \text{ cm}\cdot\text{s}^{-1}$ 。反应器运行由时间控制器控制,单个反应周期时长为140min,其中,进水5min,曝气反应120min,沉降15min,排水和闲置共5min。排水比设为3/4。反应器置于恒温水浴箱中,水温控制在 $28\sim 30^\circ\text{C}$ 。

1.3 进水水质

反应器进水采用无机人工配水,以氯化铵作为氮源,投加碳酸氢钠提供碳源和碱度,其他组分还包括 KH_2PO_4 $41 \text{ mg}\cdot\text{L}^{-1}$ 、 $\text{MgSO}_4\cdot 7\text{H}_2\text{O}$ $20 \text{ mg}\cdot\text{L}^{-1}$ 和适量微量元素^[12],pH值为 $7.8\sim 8.2$ 。在运行期间,反应器进水氨氮浓度从 $100 \text{ mg}\cdot\text{L}^{-1}$ 逐步提高至 $900 \text{ mg}\cdot\text{L}^{-1}$,对应的NLR范围为 $0.74\sim 6.66 \text{ kg}\cdot(\text{m}^3\cdot\text{d})^{-1}$,详见表1。

表1 不同运行阶段,SBR反应器的进水水质

阶段	运行时间 /d	进水 NH_4^+ -N浓度 / $\text{mg}\cdot\text{L}^{-1}$	进水 NH_4^+ -N负荷 / $\text{kg}\cdot(\text{m}^3\cdot\text{d})^{-1}$
I	0~40	100~400	0.74~2.96
II	41~75	400~600	2.96~4.44
III	76~110	600~800	4.44~5.95
IV	111~130	800~900	5.95~6.66

1.4 分析方法

混合液悬浮固体(MLSS)和挥发性悬浮固体(MLVSS)浓度采用标准重量法测定。SVI值、 NH_4^+ -N、 NO_2^- -N和 NO_3^- -N等指标分别采用30min沉降法、密闭消解-分光光度法、纳氏试剂比色法、N-(1-萘基)-乙二胺光度法和紫外分光光度法进行测定。水中游离氨(FA)与游离亚硝酸(FNA)浓度的计算公式参见文献[13]。溶液pH和溶解氧(DO)浓度分别使用PB-10型pH计(Sartorius公司)和H1946N型溶解氧测定仪(WTW公司)进行测定。采用甲醛-NaOH法对颗粒污泥中的胞外聚合物(EPS)进行提取,并使用改进的Lowry法、苯酚-硫酸法分别测定蛋白质(PN)和聚多糖(PS)组分的含量。采用OLYMPUS CX41型显微镜观察并记录颗粒形态大小的变化。

采用筛分法测算颗粒污泥的粒径分布情况。定期从反应器中取出部分污泥样品,经0.9%NaCl溶液反复清洗后,依次通过孔径为1.0、0.8、0.5、0.3、0.2mm的分样筛,称量各筛网截留的污泥质量。根据样品总质量,计算各粒径区间所占比例和颗粒平均粒径。

采用批次实验,测定污泥的氨氮比降解速率 $q(\text{NH}_4^+$ -N)、亚硝态氮比累积速率 $q(\text{NO}_2^-$ -N)、硝态氮比累积速率 $q(\text{NO}_3^-$ -N),溶液中初始氨氮浓度与各阶段反应器进水相同,具体计算方法详见文献[14]。

1.5 修正的Logistic模型

采用修正的Logistic模型对污泥平均粒径的增长过程进行拟合,如下所示:

$$D(t) = D_{\max} / [1 + e^{-k(t-t_0)}]$$

式中, t 为反应器运行时间,d; $D(t)$ 为好氧颗粒污泥的平均粒径, μm ; D_{\max} 为好氧颗粒污泥最大的平均粒径, μm ; t_0 为反应器运行滞后时间,d; k 为好氧颗粒污泥粒径的比增长速率, d^{-1} 。

2 结果与讨论

2.1 反应器的启动过程

依据NLR,将反应器运行过程(130d)分为4个

阶段,如图 1~3 所示. 在第 I 阶段(第 1~40 d),反应器的 NLR 提高了近 4 倍, $\text{NH}_4^+ \text{-N}$ 去除率在经历一定的波动后最终升至 80%, 出水 $\text{NO}_2^- \text{-N}$ 浓度持续增大, NAR 在 85%~90% 之间. 同期, MLSS 浓度增长近 20 倍, 但颗粒平均粒径变化较小. 在第 II 阶段末尾, NLR 提高至 $4.44 \text{ kg} \cdot (\text{m}^3 \cdot \text{d})^{-1}$, $\text{NH}_4^+ \text{-N}$ 去除率在经历突然下降后逐渐回升至 97%, 出水 NAR 则稳定在 80%~85% 之间. 同时, 反应器内 MLSS 浓度进一步增长, 但颗粒平均粒径却大幅缩小至约 $320 \mu\text{m}$. 在第 III 阶段初期(第 76~80 d), 较高的 NLR 对反应器性能造成了一定的冲击, $\text{NH}_4^+ \text{-N}$ 去除率在第 95 d 降至 61%, 但随后又恢复至 95% 以上. 同时, 反应器内 MLSS 浓度升至接种污泥的 82 倍, 颗粒粒径呈现缓慢增长趋势. 随着 NLR 最终达到 $6.66 \text{ kg} \cdot (\text{m}^3 \cdot \text{d})^{-1}$ (第 IV 阶段), $\text{NH}_4^+ \text{-N}$ 去除率、NAR 和 MLSS 浓度分别稳定在 90%、83% 和 $11.8 \text{ g} \cdot \text{L}^{-1}$. NGS 趋于成熟, 平均粒径约为 $420 \mu\text{m}$.

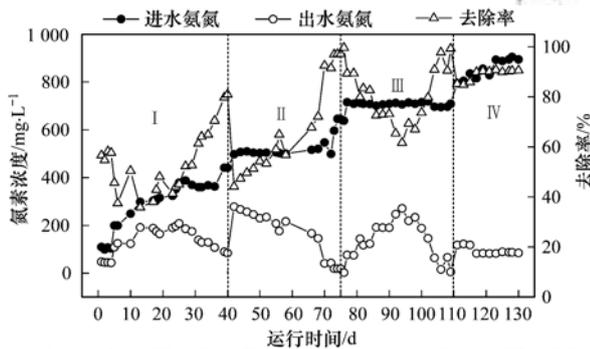


图 1 反应器对 $\text{NH}_4^+ \text{-N}$ 去除效能随运行时间的变化过程
Fig. 1 $\text{NH}_4^+ \text{-N}$ removal performance of SBR throughout the operation period

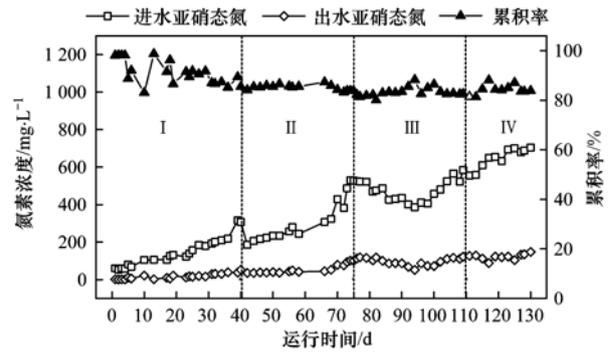


图 2 $\text{NO}_2^- \text{-N}$ 累积性能随运行时间的变化过程
Fig. 2 $\text{NO}_2^- \text{-N}$ accumulation performance of SBR throughout the operation period

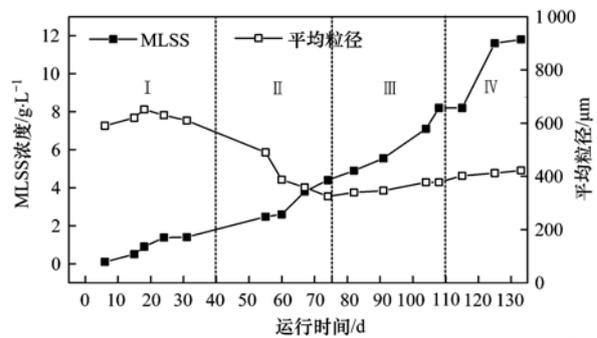


图 3 MLSS 浓度和平均粒径随运行时间的变化过程
Fig. 3 Variation of MLSS and mean average diameter throughout the operation period

在本研究中, NGS 反应器实现的最大亚硝态氮累积负荷约为 $4.9 \text{ kg} \cdot (\text{m}^3 \cdot \text{d})^{-1}$, 明显高于已有报道中的 $0.06 \sim 3.1 \text{ kg} \cdot (\text{m}^3 \cdot \text{d})^{-1}$, 如表 2 所示. 需要注意的是, 尽管 Bartroli 等^[15] 利用连续流颗粒污泥反应器获得的亚硝态氮累积负荷约为本研究最大值的 1.2 倍, 但其启动过程长达 280 d.

表 2 不同类型亚硝化反应器的性能比较

Table 2 Performance comparison between various types of nitrosation reactors

序号	反应器类型	进水 $\text{NH}_4^+ \text{-N}$ 负荷 $/\text{kg} \cdot (\text{m}^3 \cdot \text{d})^{-1}$	$\text{NH}_4^+ \text{-N}$ 去除率 /%	$\text{NO}_2^- \text{-N}$ 累积速率 $/\text{kg} \cdot (\text{m}^3 \cdot \text{d})^{-1}$	文献
1	CSTR	0.36	95	0.29	[16]
2	ALR	0.4	66	0.26	[17]
3	SBR	0.07	98	0.06	[18]
4	SBR	1.6	58	0.93	[19]
5	SBR	0.45	99	0.37	[7]
6	CSTR	3.8	58	2.1	[20]
7	SWBR	5.9	53	3.1	[21]
8	CSTR	6.1	98	6.0	[15]
9	SBR	6.6	90	4.9	本研究

1) SBR: sequencing biological reactor, 序批式反应器; CSTR: continuous stirred tank reactor, 连续流搅拌釜反应器; SWBR: swim-bed reactor, 摇床反应器; ALR: air lift reactor, 气提式反应器

2.2 颗粒污泥的形态演化

图 2 给出了反应器运行期间, 好氧颗粒污泥外

观形态的演化过程. 在第 I 阶段, 颗粒污泥的粒径较大, 呈椭球形, 表面较光滑, 密度度较好 [图 4

(a)]. 随着 NLR 的逐渐提高,污泥表面出现大量丝状物,结构变得更加松散[图 4(b)]. 在水力剪切的作用下,部分大粒径污泥可能会破碎生成更小的颗

粒. 随后,污泥表面丝状物不断裹夹、包覆,颗粒结构变得更加密实[图 4(c)]. 当 NGS 趋于成熟时,颗粒呈现光滑、规则的球形[图 4(d)].

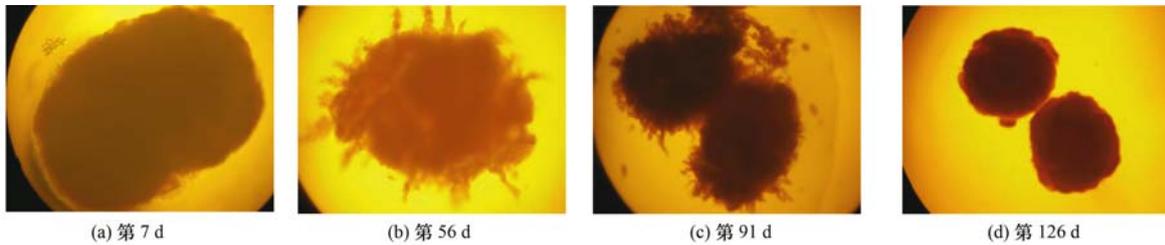


图 4 不同运行阶段,亚硝化颗粒污泥的形态照片(显微镜放大 40 倍)

Fig. 4 Morphological images of NGS during different operation periods (microscopic photos $\times 40$ times)

作为维持微生物聚集体形态稳定的重要结构性物质,EPS 的组成与颗粒污泥形态密切相关^[22]. 在本研究中,反应器内较大的上升气速和充足的氮源供给均能有效促进微生物对 EPS 的分泌,较高的 EPS 含量也有利于 AOB 等自养微生物在颗粒表面的固着^[23]. 由图 5 可知,EPS 中 PN 含量在第 I ~ III 阶段内都呈现较快增长,而 PS 含量在第 II 阶段即趋于平稳. 在异养型颗粒污泥的培养过程中也有类似情况,较高的 PN 含量有助于增强颗粒表面疏水性、改善污泥沉降性能^[24,25]. 在第 IV 阶段,成熟 NGS 中的 EPS 含量达到了 $192.2 \text{ mg}\cdot\text{g}^{-1}$,约为接种污泥的 2.7 倍,两者的 PN/PS 比值均为 2.1 左右.

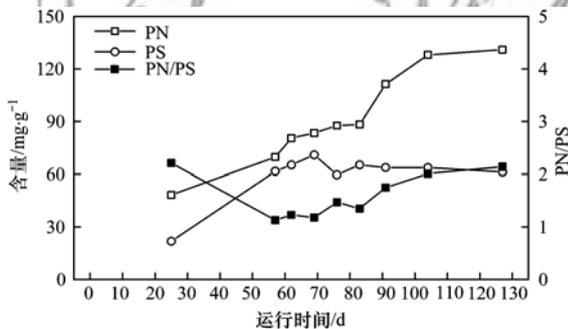


图 5 NGS 中胞外聚合物组分含量随运行时间的变化过程

Fig. 5 Variations in the "extracellular polymeric substances content" of NGS throughout the operation period

2.3 颗粒粒径的增长规律

考虑到 AOB 较慢的生长速率,本研究中 SBR 的沉降时间设置为 15 min,这有助于截留粒径较小、沉降性能较差的污泥组分. 在第 II 阶段,粒径 $< 200 \mu\text{m}$ 的污泥数量迅速增殖,导致颗粒平均粒径大幅降低(粒径分布结果未给出). 大约在第 70 d 后,颗粒平均粒径才出现增长. 采用修正的 Logistic 模型,对第 III、IV 阶段 NGS 平均粒径的变化过程进行拟合,结果如图 6 所示. 在高 NLR 条件下,NGS 平均粒径的比增长速率 k 值约为 0.0229 d^{-1} ,明显低于

以乙酸盐为生长基质的异养型颗粒污泥的 0.0539 d^{-1} ^[26],但仍比 Chen 等^[27]报道的硝化颗粒污泥 k 值 (0.0196 d^{-1}) 高出了约 17%.

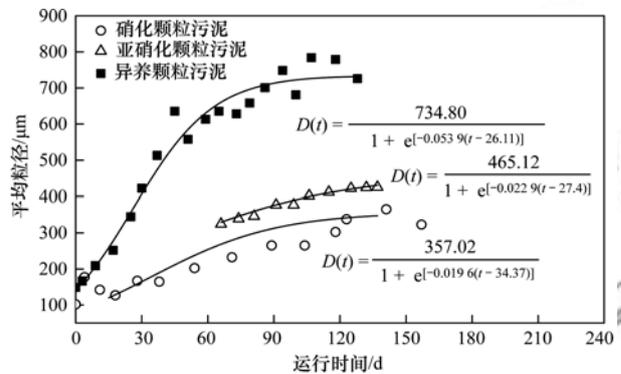


图 6 采用修正 Logistic 模型对不同种好氧颗粒污泥平均粒径增长过程的拟合结果

Fig. 6 Fitting of the average diameter growth of different types of aerobic granular sludge using modified logistic model

2.4 亚硝化系统的稳定性分析

如前所述,AOB 的有效富集与 NOB 的选择性抑制是实现稳定亚硝化反应的先决条件. 通过测定各阶段污泥的 $q(\text{NH}_4^+ - \text{N})$ 、 $q(\text{NO}_2^- - \text{N})$ 和 $q(\text{NO}_3^- - \text{N})$ 值,可以了解两类功能菌的活性变化情况.

从图 7 可知,尽管 NGS 的 $q(\text{NH}_4^+ - \text{N})$ 值随运行时间由 $51.9 \text{ mg}\cdot(\text{g}\cdot\text{h})^{-1}$ 下降至 $40.9 \text{ mg}\cdot(\text{g}\cdot\text{h})^{-1}$ (以 MLVSS 计,下同),但仍明显高于文献中的典型范围 [$13.2 \sim 33.6 \text{ mg}\cdot(\text{g}\cdot\text{h})^{-1}$]^[3, 7, 15]. 这意味着颗粒污泥始终具有很高的氨氧化活性,反应器内生物量的持续增长是获得高 $\text{NH}_4^+ - \text{N}$ 去除率的主要原因. 另外,由于 $q(\text{NO}_3^- - \text{N})$ 值从 $2.7 \text{ mg}\cdot(\text{g}\cdot\text{h})^{-1}$ 上升至 $7.7 \text{ mg}\cdot(\text{g}\cdot\text{h})^{-1}$,成熟 NGS 的 $q(\text{NO}_2^- - \text{N})/q(\text{NO}_3^- - \text{N})$ 比值(4.7)较接种污泥(18.4)明显减小.

有研究表明,对于序批式反应过程,较高的 FA 和 FNA 浓度可以对 NOB 起到联合抑制作用^[28]. 如

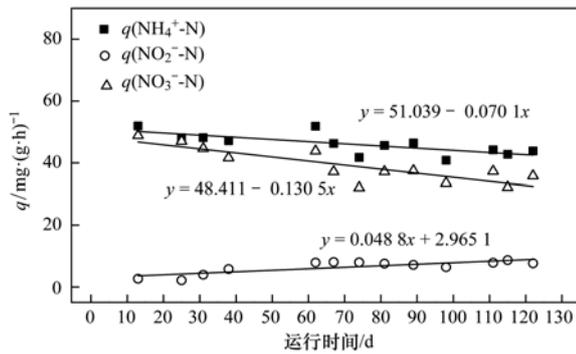


图7 NGS对不同氮素比降解/比累积速率随运行时间的变化过程

Fig. 7 Variations in specific nitrogen removal or accumulation rates of NGS throughout the operation period

图8所示,反应(曝气)期间,FA与FNA浓度分别在 $1.2 \sim 73.1 \text{ mg} \cdot \text{L}^{-1}$ 、 $0.003 \sim 0.23 \text{ mg} \cdot \text{L}^{-1}$ 内波动,两者均明显高于NOB受抑制的阈值 $0.1 \sim 1 \text{ mg} \cdot \text{L}^{-1}$ 和 $0.003 \sim 0.02 \text{ mg} \cdot \text{L}^{-1}$ [1,6].

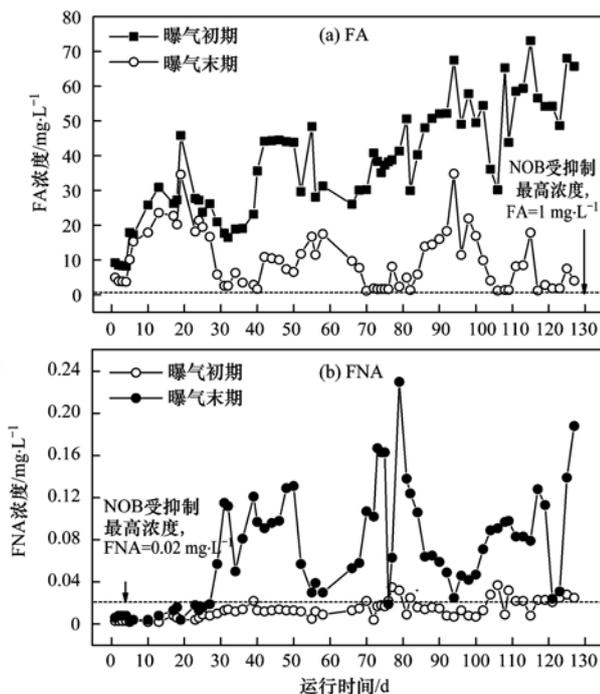


图8 在SBR运行过程中,曝气反应始末点的FA、FNA浓度水平

Fig. 8 FA and FNA concentration levels at the initial and terminal phases of aerobic reactions in SBR

另外,由于AOB对氧的亲合力较NOB更强,因此,控制较低的DO条件已成为运行各类亚硝化反应器的常用措施 [15,16]. Vázquez-Padín等 [19] 与Rathnayaka等 [29] 认为DO在好氧颗粒污泥表面渗透深度的典型范围为 $75 \sim 200 \mu\text{m}$. 在本研究中,较高的上升气速使得SBR曝气阶段的DO浓度达到 $4 \sim 6 \text{ mg} \cdot \text{L}^{-1}$. 对于平均粒径仅 $420 \mu\text{m}$ 的NGS而言,

生长于AOB内侧的NOB也能获得较为充足的DO, $q(\text{NO}_3^- \text{-N})$ 值的缓慢上升导致反应器出水NAR难以进一步提升.

3 结论

(1) 在130 d内,通过将NLR从 $0.74 \text{ kg} \cdot (\text{m}^3 \cdot \text{d})^{-1}$ 逐步提高至 $6.66 \text{ kg} \cdot (\text{m}^3 \cdot \text{d})^{-1}$,使反应器内污泥浓度增长了近118倍,出水NAR始终高于80%,亚硝态累积负荷达到 $4.9 \text{ kg} \cdot (\text{m}^3 \cdot \text{d})^{-1}$. 这意味着在适宜条件下,接种极少量种污泥也能实现高性能NGS反应器的启动.

(2) 依据Logistic模型的拟合结果,当NLR高于 $4.44 \text{ kg} \cdot (\text{m}^3 \cdot \text{d})^{-1}$ 时,污泥平均粒径的比增长速率($k=0.0229 \text{ d}^{-1}$)介于硝化颗粒污泥与异养颗粒污泥之间. 在保持较高的水力剪切与排水比的条件下,获得的成熟NGS呈现规则球形,密实度良好,其EPS含量约为接种污泥的2.7倍.

(3) 在运行期间,NGS始终具有很高的氢氧化活性, $q(\text{NH}_4^+ \text{-N})$ 值在 $40.9 \sim 51.9 \text{ mg} \cdot (\text{g} \cdot \text{h})^{-1}$ 之间. 在序批式反应中,较高的游离氨(FA)和游离亚硝酸(FNA)浓度可以对NOB起到联合抑制作用,但反应器内较高的DO浓度和较小的颗粒尺寸不利于出水NAR的进一步提升.

参考文献:

- [1] Sinha B, Annachatre A P. Partial nitrification-operational parameters and microorganisms involved [J]. Reviews in Environmental Science and Bio/Technology, 2007, 6(4): 285-313.
- [2] Corsino S F, Capodici M, Morici C, et al. Simultaneous nitrification-denitrification for the treatment of high-strength nitrogen in hypersaline wastewater by aerobic granular sludge [J]. Water Research, 2016, 88: 329-336.
- [3] Isanta E, Reino C, Carrera J, et al. Stable partial nitrification for low-strength wastewater at low temperature in an aerobic granular reactor [J]. Water research, 2015, 80: 149-158.
- [4] Grady Jr C P L, Daigger G T, Love N G, et al. Biological wastewater treatment [M]. Boca Raton, FL: CRC Press, 2011.
- [5] Gao D W, Yuan X J, Liang H, et al. Comparison of biological removal via nitrite with real-time control using aerobic granular sludge and flocculent activated sludge [J]. Applied Microbiology and Biotechnology, 2011, 89(5): 1645-1652.
- [6] Ganigué R, Volcke E I P, Puig S, et al. Impact of influent characteristics on a partial nitrification SBR treating high nitrogen loaded wastewater [J]. Bioresource Technology, 2012, 111: 62-69.
- [7] Cydzik-Kwiatkowska A, Wojnowska-Baryła I. Nitrifying granules cultivation in a sequencing batch reactor at a low organics-to-total nitrogen ratio in wastewater [J]. Folia Microbiologica, 2011, 56(3): 201-208.
- [8] Wu L, Peng C Y, Peng Y Z, et al. Effect of wastewater COD/N

- ratio on aerobic nitrifying sludge granulation and microbial population shift[J]. *Journal of Environmental Sciences*, 2012, **24**(2): 234-241.
- [9] Wang J F, Qian F Y, Liu X P, *et al.* Cultivation and characteristics of partial nitrification granular sludge in a sequencing batch reactor inoculated with heterotrophic granules [J]. *Applied Microbiology and Biotechnology*, 2016, **100**(21): 9381-9391.
- [10] Wan C L, Sun S P, Lee D J, *et al.* Partial nitrification using aerobic granules in continuous-flow reactor: rapid startup [J]. *Bioresource Technology*, 2013, **142**: 517-522.
- [11] 刘文如, 阴方芳, 丁玲玲, 等. 选择性排泥改善颗粒污泥亚硝化性能的研究[J]. *中国环境科学*, 2014, **34**(2): 396-402.
- Liu W R, Yin F F, Ding L L, *et al.* Improved nitrification performance by selective sludge discharge in aerobic granular sludge process [J]. *China Environmental Science*, 2014, **34**(2): 396-402.
- [12] 刘小鹏, 钱飞跃, 王建芳, 等. nZVI 对亚硝化颗粒污泥性能的冲击性影响研究[J]. *环境科学学报*, 2016, **36**(5): 1622-1629.
- Liu X P, Qian F Y, Wang J F, *et al.* The effect of nanoscale Zero-Valent Iron on the performance of nitrosation granular sludge [J]. *Acta Scientiae Circumstantiae*, 2016, **36**(5): 1622-1629.
- [13] Ford D L, Churchwell R L, Kachtick J W. Comprehensive analysis of nitrification of chemical processing wastewaters [J]. *Journal (Water Pollution Control Federation)*, 1980, **52**(11): 2726-2746.
- [14] 王书永, 钱飞跃, 王建芳, 等. 有机物对亚硝化颗粒污泥中功能菌活性的影响[J]. *环境科学*, 2017, **38**(1): 269-275.
- Wang S Y, Qian F Y, Wang J F, *et al.* Impact of biodegradable organic matter on the functional microbe activities in partial nitrification granules [J]. *Environmental Science*, 2017, **38**(1): 269-275.
- [15] Bartolí A, Pérez J, Carrera J. Applying ratio control in a continuous granular reactor to achieve full nitrification under stable operating conditions [J]. *Environmental Science & Technology*, 2010, **44**(23): 8930-8935.
- [16] Peng Y Z, Guo J H, Horn H, *et al.* Achieving nitrite accumulation in a continuous system treating low-strength domestic wastewater: switchover from batch start-up to continuous operation with process control [J]. *Applied Microbiology and Biotechnology*, 2012, **94**(2): 517-526.
- [17] Jemaat Z, Suárez-Ojeda M E, Pérez J, *et al.* Partial nitrification and *o*-cresol removal with aerobic granular biomass in a continuous airlift reactor [J]. *Water Research*, 2014, **48**: 354-362.
- [18] Dobbeleers T, Daens D, Miele S, *et al.* Performance of aerobic nitrite granules treating an anaerobic pre-treated wastewater originating from the potato industry [J]. *Bioresource Technology*, 2017, **226**: 211-219.
- [19] Vázquez-Padín J R, Figueroa M, Campos J L, *et al.* Nitrifying granular systems: a suitable technology to obtain stable partial nitrification at room temperature [J]. *Separation and Purification Technology*, 2010, **74**(2): 178-186.
- [20] Qiao S, Yamamoto T, Misaka M, *et al.* High-rate nitrogen removal from livestock manure digester liquor by combined partial nitrification-anammox process [J]. *Biodegradation*, 2010, **21**(1): 11-20.
- [21] Zhang L, Yang J C, Hira D, *et al.* High-rate partial nitrification treatment of reject water as a pretreatment for anaerobic ammonium oxidation (anammox) [J]. *Bioresource Technology*, 2011, **102**(4): 3761-3767.
- [22] Adav S S, Lee D J, Show K Y, *et al.* Aerobic granular sludge: recent advances [J]. *Biotechnology Advances*, 2008, **26**(5): 411-423.
- [23] 王琰, 钱飞跃, 王建芳, 等. 亚硝化颗粒污泥中 EPS 提取方法与组成特性的比较研究 [J]. *环境科学学报*, 2015, **35**(11): 3515-3521.
- Wang Y, Qian F Y, Wang J F, *et al.* Comparative study on extraction methods and composition of extracellular polymeric substances (EPS) in granular nitrosation sludge [J]. *Acta Scientiae Circumstantiae*, 2015, **35**(11): 3515-3521.
- [24] Zhu L, Lv M L, Dai X, *et al.* Role and significance of extracellular polymeric substances on the property of aerobic granule [J]. *Bioresource Technology*, 2012, **107**: 46-54.
- [25] Xiong Y H, Liu Y. Importance of extracellular proteins in maintaining structural integrity of aerobic granules [J]. *Colloids and Surfaces B: Biointerfaces*, 2013, **112**: 435-440.
- [26] Liu Y Q, Tay J H. Variable aeration in sequencing batch reactor with aerobic granular sludge [J]. *Journal of Biotechnology*, 2006, **124**(2): 338-346.
- [27] Chen F Y, Liu Y Q, Tay J H, *et al.* Rapid formation of nitrifying granules treating high-strength ammonium wastewater in a sequencing batch reactor [J]. *Applied Microbiology and Biotechnology*, 2015, **99**(10): 4445-4452.
- [28] Kim D J, Seo D W, Lee S H, *et al.* Free nitrous acid selectively inhibits and eliminates nitrite oxidizers from nitrifying sequencing batch reactor [J]. *Bioprocess and Biosystems Engineering*, 2012, **35**(3): 441-448.
- [29] Rathnayake R M L D, Oshiki M, Ishii S, *et al.* Effects of dissolved oxygen and pH on nitrous oxide production rates in autotrophic partial nitrification granules [J]. *Bioresource Technology*, 2015, **197**: 15-22.

CONTENTS

Emission Characteristics of Vehicles from National Roads and Provincial Roads in China	WANG Ren-jie, WANG Kun, ZHANG Fan, <i>et al.</i> (3553)
Impact of Gustly Northwesterly Winds on Biological Particles in Winter in Beijing	YAN Wei-zhuo, WANG Bu-ying, Oscar Fajardo Montana, <i>et al.</i> (3561)
Characteristics of Particulate Matter and Carbonaceous Species in Ambient Air at Different Air Quality Levels	FANG Xiao-zhen, WU Lin, ZHANG Jing, <i>et al.</i> (3569)
Distribution and Health Risk Assessment of Heavy Metals in Atmospheric Particulate Matter and Dust	WANG Yong-xiao, CAO Hong-ying, DENG Ya-jia, <i>et al.</i> (3575)
Observational Study of Air Pollution Complex in Nanjing in June 2014	HAO Jian-qi, GE Bao-zhu, WANG Zi-fa, <i>et al.</i> (3585)
Distribution Characteristics of Air Pollutants and Aerosol Chemical Components Under Different Weather Conditions in Jiaxing	WANG Hong-lei, SHEN Li-juan, TANG Qian, <i>et al.</i> (3594)
Observations of Reactive Nitrogen and Sulfur Compounds During Haze Episodes Using a Demuder-based System	TIAN Shi-li, LIU Xue-jun, PAN Yue-peng, <i>et al.</i> (3605)
Analysis of Anthropogenic Reactive Nitrogen Emissions and Its Features on a Prefecture-level City in Fujian Province	ZHANG Qian-hu, GAO Bing, HUANG Wei, <i>et al.</i> (3610)
Levels, Sources, and Health Risk Assessments of Heavy Metals in Indoor Dust in a College in the Pearl River Delta	CAI Yun-mei, HUANG Han-shu, REN Lu-lu, <i>et al.</i> (3620)
Influence of Noble Metal and Promoter Capacity in CDPF on Particulate Matter Emissions of Diesel Bus	TAN Pi-qiang, ZHONG Yi-mei, ZHENG Yuan-fei, <i>et al.</i> (3628)
Spatial Distribution, Source and Ecological Risk Assessment of Heavy Metals in the Coastal Sediments of Northern Dongying City	LIU Qun-qun, MENG Fan-ping, WANG Fei-fei, <i>et al.</i> (3635)
Remote Sensing of Chlorophyll-a Concentrations in Lake Hongze Using Long Time Series MERIS Observations	LIU Ge, LI Yun-mei, LÜ Heng, <i>et al.</i> (3645)
Analysis of Spatial Variability of Water Quality and Pollution Sources in Lihe River Watershed, Taihu Lake Basin	LIAN Hui-shu, LIU Hong-bin, LI Xu-dong, <i>et al.</i> (3657)
Distribution of Different Phosphorus Species in Water and Sediments from Gaocun to Lijin Reaches of the Yellow River	ZHAO Tun, JIA Yan-xiang, JIANG Bing-qi, <i>et al.</i> (3666)
Characterization of Phosphorus Fractions in the Soil of Water-Level-Fluctuation Zone and Unflooded Bankside in Pengxi River, Three Gorges Reservoir HUANG Jun-jie, WANG Chao, FANG Bo, <i>et al.</i> (3673)
Distribution of <i>n</i> -alkanes from Lake Wanghu Sediments in Relation to Environmental Changes	SHEN Bei-bei, WU Jing-lu, ZENG Hai-ao, <i>et al.</i> (3682)
Hydrological Performance Assessment of Permeable Parking Lots in High Water Areas	JIN Jian-rong, LI Tian, WANG Sheng-si, <i>et al.</i> (3689)
Analysis of the Characteristics of Groundwater Quality in a Typical Vegetable Field, Northern China	YU Jing, YU Min-da, LAN Yan, <i>et al.</i> (3696)
Composition, Evolution, and Complexation of Dissolved Organic Matter with Heavy Metals in Landfills	XIAO Xiao, HE Xiao-song, XI Bei-dou, <i>et al.</i> (3705)
Correlations Between Substrate Structure and Microbial Community in Subsurface Flow Constructed Wetlands	LI Zhen-ling, DING Yan-li, BAI Shao-yuan, <i>et al.</i> (3713)
Impact of Talc Ore Mining on Periphyton Community Structure and Water Environment	ZANG Xiao-miao, ZHANG Yuan, LIN Jia-ning, <i>et al.</i> (3721)
Physiological Characteristics and Nitrogen and Phosphorus Uptake of <i>Myriophyllum aquaticum</i> Under High Ammonium Conditions	LIU Shao-bo, RAN Bin, ZENG Guan-jun, <i>et al.</i> (3731)
Removal of Algal Organic Matter and Control of Disinfection By-products by Powder Activated Carbon	MIAO Yu, ZHAI Hong-yan, YU Shan-shan, <i>et al.</i> (3738)
Preparation and Pb ²⁺ Electrosorption Characteristics of Graphene Hydrogels Electrode	WANG Yao, JI Qing-hua, LI Yong-feng, <i>et al.</i> (3747)
Influence of Current Densities on Mineralization of Indole by BDD Electrode	ZHANG Jia-wei, WANG Ting, ZHENG Tong, <i>et al.</i> (3755)
Mechanism of Photochemical Degradation of MC-LR by Pyrite	ZHOU Wei, FANG Yan-fen, ZHANG Yu, <i>et al.</i> (3762)
Enhanced Treatment of Printing and Dyeing Wastewater Using H ₂ O ₂ -Biochemical Method	YUE Xiu, TANG Jia-li, YU Guang-ping, <i>et al.</i> (3769)
Effects of Influent C/N Ratios on Denitrifying Phosphorus Removal Performance Based on ABR-MBR Combined Process	WU Peng, CHENG Chao-yang, SHEN Yao-liang, <i>et al.</i> (3781)
Start-up of a High Performance Nitrosation Reactor Through Continuous Growth of Aerobic Granular Sludge	GAO Jun-jun, QIAN Fei-yue, WANG Jian-fang, <i>et al.</i> (3787)
Activated Sludge Mineralization and Solutions in the Process of Zero-Valent Iron Autotrophic Denitrification	ZHANG Ning-bo, LI Xiang, HUANG Yong, <i>et al.</i> (3793)
Analysis of Respirogram Characteristics of Filamentous Bulking Caused by Low Dissolved Oxygen	MA Zhi-bo, LI Zhi-hua, YANG Cheng-jian, <i>et al.</i> (3801)
Aerobic Degradation and Microbial Community Succession of Coking Wastewater with Municipal Sludge	LIU Guo-xin, WU Hai-zhen, SUN Sheng-li, <i>et al.</i> (3807)
Rapid Culture, Microbial Community Structure, and Diversity of High-Efficiency Denitrifying Bacteria	MENG Ting, YANG Hong (3816)
Abundance of Cell-associated and Cell-free Antibiotic Resistance Genes in Two Wastewater Treatment Systems	ZHANG Yan, CHEN Lü-jun, XIE Hui, <i>et al.</i> (3823)
Effect of Biochar on CH ₄ and N ₂ O Emissions from Lou Soil	ZHOU Feng, XU Chen-yang, WANG Yue-ling, <i>et al.</i> (3831)
Spatial Variability of C-to-N Ratio of Farmland Soil in Jiangxi Province	JIANG Ye-feng, GUO Xi, SUN Kai, <i>et al.</i> (3840)
Influence of Calcium Carbonate and Biochar Addition on Soil Nitrogen Retention in Acidified Vegetable Soil	YU Ying-liang, YANG Lin-zhang, Alfred Oduor Odindo, <i>et al.</i> (3451)
Comparison of Soil Hydraulic Characteristics Under the Conditions of Long-term Land Preparation and Natural Slope in Longtan Catchment of the Loess Hilly Region FENG Tian-jiao, WEI Wei, CHEN Li-ding, <i>et al.</i> (3860)
Effects of Organic Carbon Content on the Residue and Migration of Polycyclic Aromatic Hydrocarbons in Soil Profiles FEI Jia-jia, ZHANG Zhi-huan, WAN Tian-tian, <i>et al.</i> (3871)
Major Factors Influencing the Cd Content and Seasonal Dynamics in Different Land Cover Soils in a Typical Acid Rain Region	LIU Xiao-li, ZENG Zhao-xia, TIE Bai-qing, <i>et al.</i> (3882)
Application Potential and Assessment of Metallurgical Contaminated Soil After Remediation in Tongguan of Shaanxi	WANG Jiao, XIAO Ran, LI Rong-hua, <i>et al.</i> (3888)
Effects and Mechanisms of In-situ Cement Solidification/Stabilization on a Pb-, Zn-, and Cd-Contaminated Site at Baiyin, China	LÜ Hao-yang, FEI Yang, WANG Ai-qin, <i>et al.</i> (3897)
Concentrations and Health Risk Assessment of Polycyclic Aromatic Hydrocarbons (PAHs) in Soils and Vegetables influenced by Facility Cultivation JIN Xiao-pei, JIA Jin-pu, BI Chun-juan, <i>et al.</i> (3907)
Effects of Arbuscular Mycorrhizal Fungi on the Growth and Uptake of La and Pb by Maize Grown in La and Pb-Contaminated Soil	CHANG Qing, GUO Wei, PAN Liang, <i>et al.</i> (3915)
Effects of Straw Incorporation on Cadmium Accumulation and Subcellular Distribution in Rice	DUAN Gui-lan, WANG Fang, CEN Kuang, <i>et al.</i> (3927)
Redox Transformation of Arsenic and Antimony in Soils Mediated by <i>Pantoea</i> sp. IMH ZHANG Lin, LU Jin-suo (3937)
Adsorption Characteristics of Biochar on Heavy Metals (Pb and Zn) in Soil	WANG Hong, XIA Wen, LU Ping, <i>et al.</i> (3944)
Characteristics of <i>Enteromorpha prolifera</i> Biochars and Their Adsorption Performance and Mechanisms for Cr(VI)	CHEN You-yuan, HUI Hong-xia, LU Shuang, <i>et al.</i> (3953)
External Phosphorus Adsorption and Immobility with the Addition of Ignited Water Purification Sludge	YU Sheng-nan, LI Yong, LI Da-peng, <i>et al.</i> (3962)
Preparation of Adsorption Ceramsite Derived from Sludge Biochar	LI Jie, PAN Lan-jia, YU Guang-wei, <i>et al.</i> (3970)
Construction of Graphitic Carbon Nitride-Bismuth Oxide Layered Heterostructures and Their Photocatalytic Antibacterial Performance HUANG Jian-hui, LIN Wen-ting, XIE Li-yan, <i>et al.</i> (3979)